V International Conference on Computational Methods for Coupled Problems in Science and Engineering
COUPLED PROBLEMS 2013
S. Idelsohn, M. Papadrakakis and B. Schrefler (Eds)

PREDICTION OF SOUND FIELDS IN ACOUSTIC CAVITIES COUPLED TO ABSORPTIVE STRUCTURES DUE TO VIBRATING SURFACES

MARTIN BUCHSCHMID*, GERHARD MÜLLER* AND MARTINA POSPIECH†

*Chair of Structural Mechanics
Technische Universität München
Arcisstrasse 21, 80333 Munich, Germany
e-mail: martin.buchschmid@tum.de, web page: http://www.bm.bv.tum.de

†Bertrandt Ingenieurbüro GmbH
Anton-Ditt-Bogen 16, 80939 Munich, Germany
e-mail: martina.pospiech@partner.bmw.de, web page: http://www.bertrandt.com

Key words: Room Acoustics, Fluid Structure Interaction, Component Mode Synthesis, Integral Transform Methods

Abstract. In the scope of this contribution a model for the Fluid Structure Interaction (FSI) is presented, where absorptive structures can be considered. A special focus is layed on the interface coupling modes between absorber and fluid. For the simulation of the spatial resolution of the sound field within acoustic cavities techniques based on Finite Element formulations are used. To reduce the number of degrees of freedom a model reduction method, based on a Component Mode Synthesis (CMS), is applied. The cavity boundary conditions, e.g. compound absorbers made of homogenous plates and porous foams, are modeled using Integral Transform Methods (ITM) and appropriate material formulations. Wavenumber dependent impedances are computed for the absorptive structure and used for the coupling with the acoustic cavity adding interface coupling modes for the fluid and applying Hamilton's principle.

1 INTRODUCTION

Due to increasing requirements of comfort, acoustic design has become more important during the last years, especially in the field of civil engineering and automotive design. The sound field within rooms or vehicles has to be predicted in the scope of the design process for the specific use.

The calculation of the sound pressure level inside of acoustic cavities is usually done with the help of the Statistical Energy Analysis (SEA). This method is robust for systems

with a high modal density and it is based on an averaging over frequency bands, points of excitation and points of observation. However, its performance is limited if a description of the spatial resolution of the response is necessary and if the influence of boundary conditions has to be described in detail.

In the scope of the acoustic design of rooms or vehicles elements like reflectors or absorbers are placed into the sound field. Therefore a robust method for the phase correct modeling of interior sound fields with sufficient spatial resolution is needed for the relevant mechanisms of excitation, where the absorptive behavior of the delimiting surfaces can be considered. Methods, based on Finite Element formulations are used for this purpose.

Finite Element models for absorptive boundary conditions in acoustical calculations lead to a huge number of degrees of freedom. In order to reduce this number of unknowns an impedance approach considering a wavenumber dependent impedance is used for plate-like compound absorbers to introduce varying angles of incidence for the sound wave. The coupling modes used for the FSI of acoustic fluid and absorber are discussed in detail, where a method for the estimation of the number of modes, which have to be considered, is presented. Finally a numerical example for the coupled system is presented.

2 FLUID STRUCTURE INTERACTION

The derivation of the FSI method is carried out in the frequency domain. Therefore only excitations, harmonically oscillating in time, with the circular frequency of excitation Ω are considered. Consequently the steady state solution for both state variables pressure p_A and sound velocity $\mathbf{v}_A$ is harmonic in time.

2.1 Hamilton's Principle and Ritz Approach

For the vibro-acoustical problem discussed in this contribution a description of Hamilton's principle, which is based on velocities, is applied. The structure is divided into substructures (see figure 1), where the acoustic fluid and the boundary conditions are defined as subsystems respectively. According to Hamilton's principle equilibrium is fulfilled by the velocity field, which meets the kinematic boundary conditions, the conditions at $t = t_1$ and $t = t_2$ and, in addition to that, satisfies

$$\int_{t_1}^{t_2} \delta\Big(L_A(t) + L_{BC}(t, Z) + \mathbf{R}^T \boldsymbol{\lambda}(t)\Big) + \delta W_{BC}^{nc}(t, Z) + \delta W_{Load}^{nc}(t)\, dt = 0. \tag{1}$$

The Lagrangian function L_A for the acoustic fluid results from the kinetic energy T_A and the potential energy U_A

$$L_A(t) = T_A(t) - U_A(t), \tag{2}$$

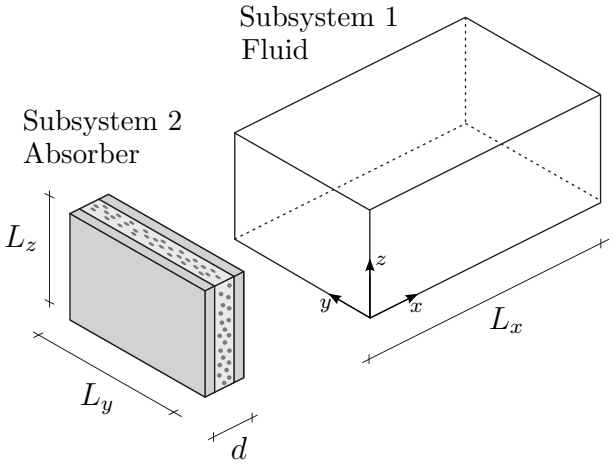

Figure 1: Subsystem definition

where the energies are computed out of

$$T_A(t) = \frac{\rho_A}{2} \int\limits_V |\mathbf{v}_A(\mathbf{x},t)|^2 dV \qquad \text{and} \qquad U_A(t) = \frac{1}{2\rho_A c_A^2} \int\limits_V |p_A(\mathbf{x},t)|^2 dV$$

respectively. Harmonically oscillating loads or excitations via surfaces are considered in Hamilton's Principle as a non conservative forces by their virtual work δW^{nc}_{Load}

$$\delta W^{nc}_{Load}(t) = \int\limits_{A_{Load}} p_{Load}(\mathbf{x},t)\, \mathbf{n}_{Load}(\mathbf{x})\, \delta\mathbf{w}(\mathbf{x},t)\; dA. \tag{3}$$

The formulation of L_{BC} and δW^{nc}_{BC} will be given for a wavenumber-dependent impedance in the following section. In the scope of a Ritz approach a linear equation system is obtained to compute the unknown coefficients.

2.2 Component Mode Synthesis

The Component Mode Synthesis (CMS) is a substructuring technique for large coupled problems, which was introduced by Hurty [5] to reduce the number of unknowns while keeping the physical characteristics of the structure. In contrast to Hurty, the CMS is used based on a modal description in the scope of this method. In order to model arbitrary geometries for the acoustic fluid a numerical approach based on the Spectral Finite Element Method (SFEM) [6, 4] is used. In the frame of the CMS the superscript N stands for normal modes and the superscript C for coupling modes. Normal modes are the eigenmodes of the air volume enclosed by totally reflecting boundaries and coupling modes are additionally introduced to provide the coupling to other boundary conditions, like a deformable structure, an absorber or an open interface to another acoustic volume.

For the velocity $\mathbf{v}_A$ in the acoustic fluid the approach (4) is applied.

$$\mathbf{v}_A(\mathbf{x},t) = \sum_m \mathbf{v}_m^N(\mathbf{x}) \left(\mathcal{A}_m e^{i\Omega t} + \overline{\mathcal{A}}_m e^{-i\Omega t}\right) + \sum_n \mathbf{v}_n^C(\mathbf{x}) \left(\mathcal{B}_n e^{i\Omega t} + \overline{\mathcal{B}}_n e^{-i\Omega t}\right) \tag{4}$$

Assuming an acoustic fluid, the irrotational behavior of the sound velocity allows the use of a velocity potential $\Phi_A(\mathbf{x})e^{i\Omega t}$.

$$\mathbf{v}_A(\mathbf{x},t) = \operatorname{grad} \Phi_A(\mathbf{x},t)$$

Considering the steady state problem after applying a Fourier transformation from the time- to the frequency-domain, the velocity potential solves the Helmholtz equation (5), where c_A denotes the constant speed of sound.

$$\Delta\hat{\Phi}_A(\mathbf{x},\omega) + \frac{\omega^2}{c_A^2}\,\hat{\Phi}_A(\mathbf{x},\omega) = 0 \tag{5}$$

In the Fourier-transformed domain the velocity $\hat{\mathbf{v}}_A$ and the pressure $\hat{p}_A$ read as follows:

$$\hat{\mathbf{v}}_A(\mathbf{x},\omega) = \operatorname{grad} \hat{\Phi}_A(\mathbf{x},\omega) \tag{6}$$

$$\begin{aligned} \hat{p}_A(\mathbf{x},\omega) &= -\frac{\rho_A c_A^2}{i\,\omega} \operatorname{div} \hat{\mathbf{v}}_A(\mathbf{x},\omega) \\ &= -\frac{\rho_A c_A^2}{i\,\omega} \Delta\hat{\Phi}_A(\mathbf{x},\omega) \end{aligned} \tag{7}$$

The normal modes for the acoustic fluid are defined in terms of the velocity potential $\hat{\Phi}^N$ assuming fixed interfaces, which means reflective wall conditions for all boundaries of the fluid:

$$\operatorname{grad} \hat{\Phi}_m^N(\mathbf{x},\omega_m) \cdot \mathbf{n}_{BC} = 0 \tag{8}$$

The normal modes are supplemented by coupling modes in order to define a valid set of trial functions for (4). These coupling modes enable velocities perpendicular to the coupling interface and also at the location of a surface-excitation. They fulfill the reflective boundary conditions at all surfaces of the room, except for the interface defined as $\mathbf{x}_{\mathrm{BC}}$, where modal trial functions $g(\mathbf{x}_{BC})$ are prescribed

$$\operatorname{grad} \hat{\Phi}_n^C(\mathbf{x},\Omega) \cdot \mathbf{n}_{\mathrm{BC}} = g(\mathbf{x}_{\mathrm{BC}}) \tag{9}$$

leading to an inhomogeneous *Helmholtz* equation for each coupling mode. For the specification of the function $g(\mathbf{x}_{\mathrm{BC}})$ a multi-index $n = (n_1, n_2)$ is defined with respect to the prescribed vibration pattern. The coupling modes are calculated as solutions of the dynamic problem in a harmonic analysis. Thus the number of coupling modes, which is considered in the calculation, can be chosen with respect to the physical properties of the system for reasons of efficiency.

In order to exemplify the influence of the wavenumber, a rectangular room with reflective walls $[0, L_x = 6\,m] \times [0, L_y = 3\,m] \times [0, L_z = 2\,m]$ is considered and the coupling modes are calculated with the Spectral Finite Element formulation.

Figure 2 shows the velocity potential Φ^c of the holohedral coupling modes, which cover the whole wall and the subregional coupling modes, when a sinusoidal vibration pattern is prescribed at the interface with a circular frequency of excitation $\Omega = 459\,\frac{rad}{s}$.

Comparing the potential-fields for different multi-indices $n = (n_1, n_2)$ one observes far-fields for small wavenumbers in the acoustic fluid, whereas with rising wavenumbers near-field solutions are obtained. They are characterized by an exponential decaying behavior perpendicular to the interface. The impact of the subregional modes on the acoustic fluid is smaller than in case of holohedral coupling modes. Also concerning the decay characteristics one observes differences.

These near-field effects can be used to reduce the number of unknowns in the CMS approach. Focusing on the sound field in the cavity, it is sufficient to consider just the far-field coupling modes. To define a sufficient number of coupling modes for an efficient numerical computation, this effect has to be predicted with low numerical effort (a calculation of the coupling modes with the SFEM in advance in order to investigate the decay characteristics would be too expensive). Applying Integral Transform Methods and filtering techniques in the spatial domain one can estimate these decay characteristics with negligible numerical effort. Starting from the wave equation in terms of displacements

$$\frac{\partial^2 u(x,y,z,t)}{\partial x^2} + \frac{\partial^2 u(x,y,z,t)}{\partial y^2} + \frac{\partial^2 u(x,y,z,t)}{\partial z^2} = \frac{1}{c_A^2}\frac{\partial^2 u}{\partial t^2} \tag{10}$$

a *Fourier* transformation is applied assuming infinite dimensions of the interface. The spatial coordinates y and z, defining the plane of the interface, are transformed in the wavenumber domain and a transformation into the frequency domain is carried out, considering vibrations in the steady state with a circular frequency of excitation Ω:

$$\frac{\partial^2 \hat{u}(x,k_y,k_z,\Omega)}{\partial x^2} + \left[\left(\frac{\Omega}{c_A}\right)^2 - k_y^2 - k_z^2\right] \hat{u}(x,k_y,k_z,\Omega) = 0 \tag{11}$$

The ordinary differential equation (11) is solved with the exponential approach obtaining the solution for the displacement field of the homogeneous problem:

$$\hat{u}(x,k_y,k_z,\Omega) = \begin{cases} \hat{u}_0(k_y,k_z)\,\left(\frac{-e^{-\lambda L_x}}{(e^{\lambda L_x}-e^{-\lambda L_x})}e^{\lambda x} + \frac{e^{\lambda L_x}}{(e^{\lambda L_x}-e^{-\lambda L_x})}e^{-\lambda x}\right), & \lambda \neq 0 \\ \hat{u}_0(k_y,k_z)\,\left(1 - \frac{x}{L_x}\right), & \lambda = 0 \end{cases} \tag{12}$$

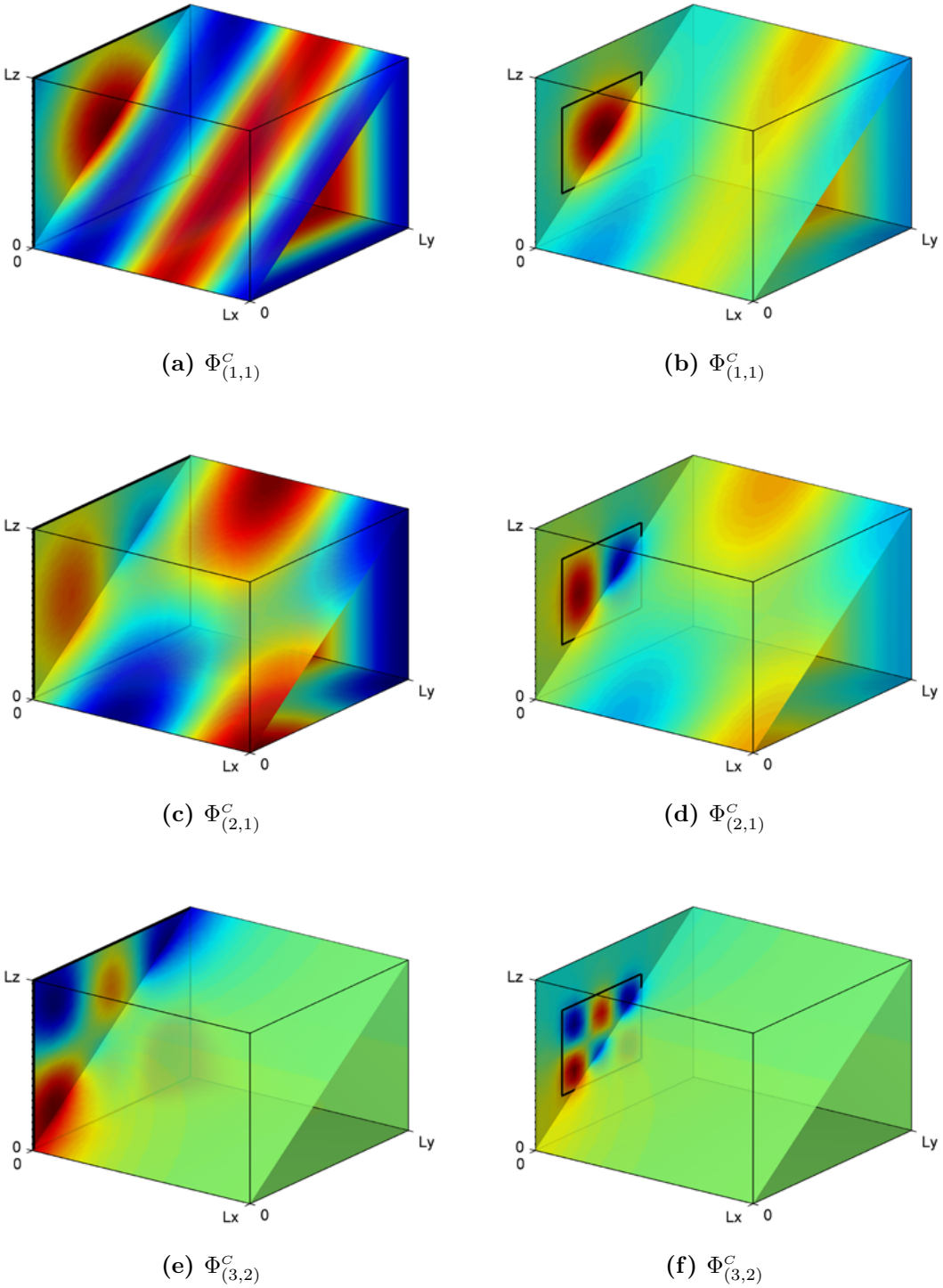

(a) $\Phi^C_{(1,1)}$ **(b)** $\Phi^C_{(1,1)}$

(c) $\Phi^C_{(2,1)}$ **(d)** $\Phi^C_{(2,1)}$

(e) $\Phi^C_{(3,2)}$ **(f)** $\Phi^C_{(3,2)}$

Figure 2: Holohedral and subregional coupling modes for the velocity potential $\Phi^C_n(\mathbf{x})$ of the rectangular room with reflective walls $[0, L_x = 6\,m] \times [0, L_y = 3\,m] \times [0, L_z = 2\,m]$ for different multi-indices $n = (n_1, n_2)$ with $\Omega = 459\,\frac{rad}{s}$

The ranges for the far-field, the near-field and the transition zone, where a linear decay is observed, are listed in (13).

$$k_y^2 + k_z^2 \begin{cases} < & \frac{\Omega^2}{c_A^2}, \quad \text{far-field} \\ > & \frac{\Omega^2}{c_A^2}, \quad \text{near-field} \\ = & \frac{\Omega^2}{c_A^2}, \quad \text{linear decay} \end{cases} \tag{13}$$

In the k_y, k_z-domain the transition zone marks a circle with the radius $\frac{\Omega}{c_A}$. In the practical problem finite absorbers with dimensions $L_x^{BC} \times L_z^{BC}$ have to be applied. Therefore the infinite vibration pattern $u_0(y,z)$ is multiplied with a rectangular filter function $\Theta(y,z)$ in the spatial domain, which is equals a convolution with a 2d $sinc-$function in the wavenumber domain.

$$\Theta(y,z) \; \circ\!\!-\!\!\bullet \; \frac{4}{k_y\, k_z} \sin\left(\frac{L_y^{BC}}{2}\, k_y\right) \sin\left(\frac{L_z^{BC}}{2}\, k_z\right) \tag{14}$$

Applying a *Fourier* transformation of the velocity pattern and evaluating the results according to condition (13) the necessary number of coupling modes can be specified. In figure 3 the results are depicted for the holohedral and the subregional coupling modes, where the magenta colored circle specifies the transition zone. The wavenumbers within this circle refer to far-field solutions.

Figure 3 shows, that for the subregional coupling modes the transition to near-fields is linked with smaller multi-index combinations than for the holohedral coupling modes, because a fixed multi-index combination results in higher wavenumbers for the subregional than for the holohedral modes. Also the effect caused by the spatial limitation of infinite vibration patterns is clearly recognized. The number of normal modes, which has to be considered, depends on the frequency of excitation Ω and on the load pattern. The number of coupling modes can be limited efficiently selecting the far-fields in the wavenumber domain.

In the following a rectangular geometry is considered for the absorptive boundary condition and $g(\mathbf{x}_{BC})$ is expressed with $\psi_n(y,z)$ for each mode, where y and z mark the local coordinates in the reference coordinate system of the absorber.

Considering the procedural method in the next steps, in especially the computation of the Lagrangian L_{BC} for the absorber out of impedances, it is advantageous to express $\psi_n(y,z)$ with its Fourier Series.

$$\hat{\psi}_n(y,z) = \sum_r \sum_s E_{nrs}\, e^{i(r\Delta k_y\, y + s\Delta k_z\, z)} \tag{15}$$

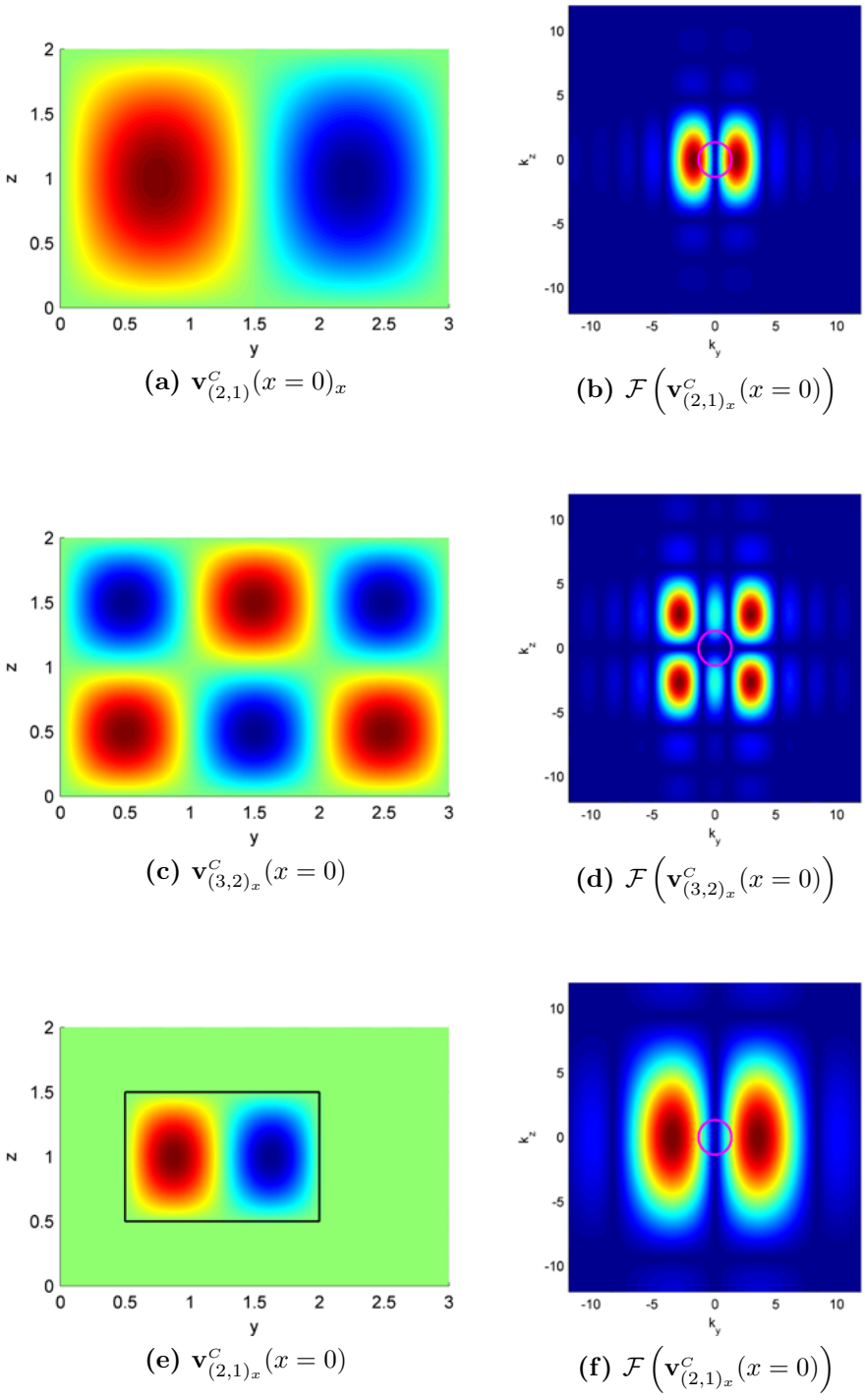

(a) $\mathbf{v}^C_{(2,1)}(x=0)_x$ **(b)** $\mathcal{F}\left(\mathbf{v}^C_{(2,1)_x}(x=0)\right)$

(c) $\mathbf{v}^C_{(3,2)_x}(x=0)$ **(d)** $\mathcal{F}\left(\mathbf{v}^C_{(3,2)_x}(x=0)\right)$

(e) $\mathbf{v}^C_{(2,1)_x}(x=0)$ **(f)** $\mathcal{F}\left(\mathbf{v}^C_{(2,1)_x}(x=0)\right)$

Figure 3: Near-field effects of the holohedral and subregional coupling modes

Thus the trial function at the interface is specified for an absorptive boundary condition as

$$\hat{v}_{BC}(y,z,t) = \sum_n \hat{\psi}_n(y,z) \left(\mathcal{C}_n e^{i\Omega t} + \overline{\mathcal{C}}_n e^{-i\Omega t} \right). \tag{16}$$

Carrying out the integration required in equation (1) over one period of the steady state vibration one obtains the Lagrangian L_{BC} and the virtual work of the non conservative forces δW_{BC}. In this short essay we focus on trial functions, where due to reasons of orthogonality the off diagonal terms vanish.

$$\int_0^T L_{BC}\, dt = \frac{T}{\Omega} L_y\, L_z \left[\sum_n \mathcal{C}_n \overline{\mathcal{C}}_n \sum_r \sum_s \mathrm{Im}\left(Z\left(r,s,\Omega\right)\right) \left|E_{nrs}\right|^2 \right] \tag{17}$$

$$\int_0^T \delta W_{BC}\, dt \;=\; -\frac{T}{i\Omega} L_y\, L_z \sum_n \left(\overline{\mathcal{C}}_n \delta \mathcal{C}_n - \mathcal{C}_n \delta \overline{\mathcal{C}}_n \right) \sum_r \sum_s \mathrm{Re}\left(Z\left(r,s,\Omega\right)\right) \left|E_{nrs}\right|^2 \tag{18}$$

In case of sinusoidal functions also the Fourier approximation $\hat{\psi}_n(y,z)$ can be omitted. A detailed discussion as well as the expressions for a general definition of the trial functions are presented in [2]. With the imaginary part of the impedance $\mathrm{Im}\left(Z\left(r,s,\Omega\right)\right)$ the flexible characteristics of the absorber can be modeled, as shown above. The absorptive characteristics are expressed by the real part of impedance $\mathrm{Re}\left(Z\left(r,s,\Omega\right)\right)$.

A description of porous layers based on the Theory of Porous Media [1] as well as the formulation of the system of differential equations and the solution for the fundamental system in the wavenumber-frequency domain for compound absorbers is presented in detail in [2, 3].

3 COUPLING THE SUBSYSTEMS AND ASSEMBLING THE EQUATION SYSTEM

The Normal and coupling modes, which are specified in the CMS approach in equation (4), are computed for the acoustic fluid as trial functions in the scope of a Ritz approach and the Lagrangian of the fluid as well as the virtual work of the external loads are computed with equations (2) and (3) respectively. The Lagrangian of the compound absorber and the virtual work of the non-conservative damping forces are computed with (17) and (18) for instance.

The unknown complex coefficients $\mathcal{A}_i$ and $\mathcal{B}_i$ refer to the normal and the coupling modes in the acoustic volume, whereas $\mathcal{C}_i$ are the coefficients of the trial functions of the compound absorber. The coupling condition of the fluid and the absorber at the interface, which is defined in equation (1) with the help of the vector of Lagrange multipliers $\boldsymbol{\lambda}$, simply results in $\mathcal{B}_i = \mathcal{C}_i$ and $\bar{\mathcal{B}}_i = \bar{\mathcal{C}}_i$, if the same velocity pattern is chosen for the trial function of the absorber and for the boundary condition of the fluid at the absorber-interface. Thus the vectors for the unknown coefficients $\mathbf{x}$ and the corresponding conjugate

complex values $\bar{\mathbf{x}}$ read:

$$\begin{aligned} \mathbf{x} &= \begin{bmatrix} \mathcal{A}_1 \cdots \mathcal{A}_{m_{\max}} & \mathcal{B}_1 \cdots \mathcal{B}_{n_{\max}} \end{bmatrix}^T \\ \bar{\mathbf{x}} &= \begin{bmatrix} \bar{\mathcal{A}}_1 \cdots \bar{\mathcal{A}}_{m_{\max}} & \bar{\mathcal{B}}_1 \cdots \bar{\mathcal{B}}_{n_{\max}} \end{bmatrix}^T \end{aligned} \tag{19}$$

The solution of the variational problem is reduced to a problem of minimization because of the Ritz approach. It is advantageous to express the conjugate complex coefficients with real and imaginary values in order to formulate the extremal problem:

$$\begin{aligned} \mathbf{x} &= \begin{bmatrix} \mathbf{x}^R + i\,\mathbf{x}^I \end{bmatrix}^T \\ \bar{\mathbf{x}} &= \begin{bmatrix} \mathbf{x}^R - i\,\mathbf{x}^I \end{bmatrix}^T \end{aligned} \tag{20}$$

The real and imaginary parts of the complex coefficients mark the new set of unknowns $\mathbf{y} = \begin{bmatrix} \mathbf{x}^R & \mathbf{x}^I \end{bmatrix}^T$, where the total number of real valued unknowns is $2\,(m_{\max} + n_{\max})$. Here $m_{\max}$ and $n_{\max}$ are the maximum numbers of normal and coupling modes respectively.

$$\begin{aligned} \mathbf{x}^R &= \begin{bmatrix} \mathcal{A}_1^R \cdots \mathcal{A}_{m_{\max}}^R & \mathcal{B}_1^R \cdots \mathcal{B}_{n_{\max}}^R \end{bmatrix}^T \\ \mathbf{x}^I &= \begin{bmatrix} \mathcal{A}_1^I \cdots \mathcal{A}_{m_{\max}}^I & \mathcal{B}_1^I \cdots \mathcal{B}_{n_{\max}}^I \end{bmatrix}^T \end{aligned} \tag{21}$$

For the consideration of the virtual work a vector $\delta\mathbf{y}$ is specified analogously. Carrying out the minimization of the Lagrangian one obtains a system of real valued linear equations

$$\mathbf{K}\,\mathbf{y} = \mathbf{F}, \tag{22}$$

where the matrix of coefficients K_{ij} reads

$$K_{ij} = \frac{\partial^2 \int_0^T L_A \; dt}{\partial y_i \, \partial y_j} + \frac{\partial^2 \int_0^T L_{\mathrm{BC}}(Z) \; dt}{\partial y_i \, \partial y_j} + \frac{\partial^2 \int_0^T \delta W_{\mathrm{BC}}^{\mathrm{nc}}(Z) \; dt}{\partial \, \delta y_i \, \partial y_j} \tag{23}$$

and the load vector $\mathbf{F} = \begin{bmatrix} \mathbf{F}^R & \mathbf{F}^I \end{bmatrix}^T$ considers the external forces:

$$F_i = -\frac{\partial \int_0^T \delta W_{\mathrm{Load}}^{\mathrm{nc}} \; dt}{\partial \, \delta y_i} \tag{24}$$

Defining submatrices $\mathbf{K}_{rs}$ for the matrix of coefficients, equation (22) reads:

$$\begin{bmatrix} \mathbf{K}_{11} & \mathbf{K}_{12} \\ \mathbf{K}_{21} & \mathbf{K}_{22} \end{bmatrix} \begin{bmatrix} \mathbf{x}^R \\ \mathbf{x}^I \end{bmatrix} = \begin{bmatrix} \mathbf{F}^R \\ \mathbf{F}^I \end{bmatrix} \tag{25}$$

In consequence of the complex property of the unknown coefficients the relations

$$\mathbf{K}_{11} = \mathbf{K}_{22} \tag{26}$$

$$\mathbf{K}_{21} = -\mathbf{K}_{12} \tag{27}$$

hold for the submatrices.

4 NUMERICAL EXAMPLE

For arbitrary geometries the normal and coupling modes can be computed with the SFEM. The only restriction, given by the application of the ITM for the Lagrangian of the absorber, is, that the interface has to be plain. In the following a 2d acoustic volume with an inclining rear-wall is considered. The wall containing the interface could be inclined as well. The geometry of the system is sketched in figure 4, where $L_x^1 = 6\,m$, $L_x^2 = 1.5\,m$ and $L_y = 2\,m$. The model is set up with 192 spectral finite elements. The interface is covered with a $7.2\,cm$ layer of Melamine Foam. A unit point source is located at $x = 1.15\,m$ and $y = 0.77\,m$. The location is chosen under the premise of exciting nearly all modeshapes.

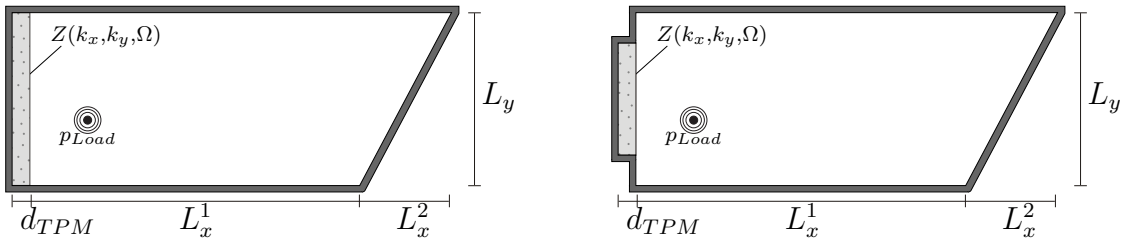

Figure 4: 2d structure with with inclined wall and porous absorber (holohedral and subregional coupling)

In figure 5 the steady state response for the sound pressure level is sketched. The different interface-specifications are compared for a frequency of excitation of $163\,Hz$. Due to the fact, that the frequency of excitation is near to a natural frequency, primarily one specific modeshape is excited, which would lead to very high sound pressures in case of an undamped system. A significant reduction is achieved due to the application of the absorptive layer at the boundary. Comparing both results in figure 5 one observes lower sound pressure levels for the holohedral case, because here the absorptive area, which is introduced into the system by the boundary condition, and therefore the dissipation of energy is higher than for subregional coupling.

5 CONCLUSION

In this contribution a method is presented to compute acoustic cavities under harmonically oscillating loads in order to get phase correct results with a spatial resolution for the sound field using a CMS approach. The normal and constraint modes for the acoustic cavity are calculated with the SFEM, where the number of necessary coupling modes is estimated in the wavenumber domain. The SFEM formulation is implemented in order to model arbitrary geometries for the acoustic cavity. Because of the Fourier transforms in the scope of the ITM however the interface has to be plane. Layered boundary structures as compound absorbers, consisting of homogeneous and porous materials, are modeled efficiently using the Fourier transform, where the number of unknowns can be reduced significantly.

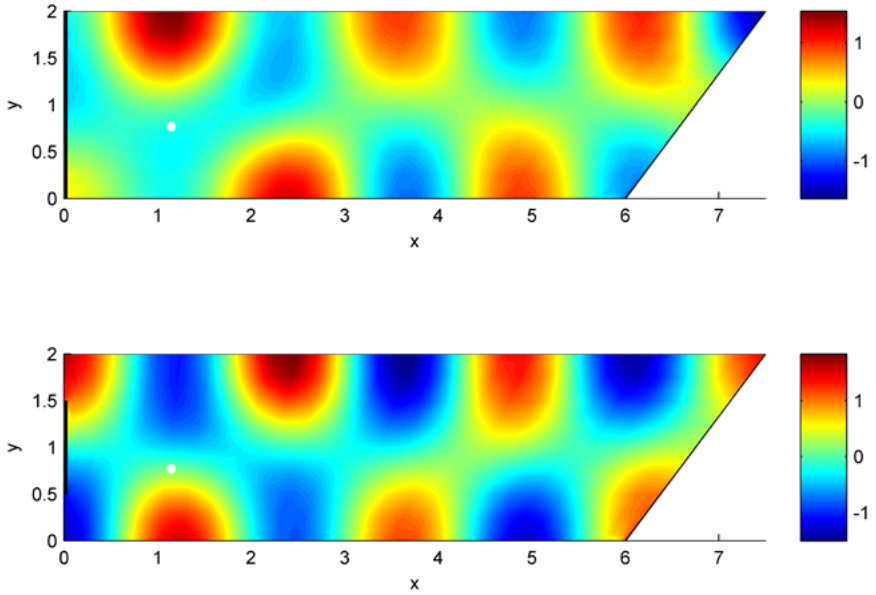

Figure 5: Sound-pressure $p(x, y)$ [Pa] for a frequency of excitation of $163\,Hz$

REFERENCES

[1] de Boer, R.: Trends in Continuum Mechanics of Porous Media. Theory and Applications of Transport in Porous Media. Springer (2005)

[2] Buchschmid, M.: ITM-based FSI-models for rooms with absorptive boundaries. Ph.D. thesis, TU München (2011)

[3] Buchschmid, M., Müller, G., Pospiech, M.: ITM-based FSI-models for room acoustical simulations. In: WCCM 2012. iacm (2012)

[4] Buchschmid, M., Pospiech, M., Müller, G.: Coupling impedance boundary conditions for absorptive structures with spectral finite elements in room acoustical simulations. Computing and Visualization in Science **13**, 355–363 (2010)

[5] Hurty, W.: Vibrations of structural systems by component-mode synthesis. Journal of Engineering Mechanics (ASCE) **86(4)**, 51–69 (1960)

[6] Pospiech, M.: Numerical simulations in room acoustics using direct coupling techniques and finite elements. Ph.D. thesis, TU München (2011)